Production of Acrylic Acid through Nickel-Mediated Coupling of Ethylene and Carbon Dioxide—A DFT Study

David C. Graham, Cassandra Mitchell, Michael I. Bruce, Gregory F. Metha, John H. Bowie, and Mark A. Buntine*

Cooperative Research Centre for Greenhouse Gas Emissions (CO2CRC), School of Chemistry and Physics, University of Adelaide, Adelaide, Australia 5005

Received June 17, 2007

The production of acrylic acid ($CH_2{=}CHCO_2H$) via homogeneous nickel-mediated coupling of ethylene ($CH_2{=}CH_2$) and carbon dioxide (CO_2) is industrially unattractive at present due to its stoichiometric, rather than catalytic, reaction profile. We utilize density functional theory (DFT) to describe the potential energy surface for both the nickel-mediated coupling reaction and an intramolecular deactivation reaction reported to hinder the desired catalytic activity. The calculated route for the catalytic production of acrylic acid can be divided into three main parts, none of which contain significantly large barriers that would be expected to prohibit the overall catalytic process. Investigation of the catalyst deactivation reaction reveals that the proposed product lies +102.6 kJ mol^{-1} above the reactants, thereby ruling out this type of pathway as the cause of the noncatalytic activity. Instead, it is far more conceivable that the overall reaction thermodynamics are responsible for the lack of catalytic activity observed, with the solvation -corrected Gibbs free energy of the coupling reaction in question (i.e., $CH_2{=}CH_2 + CO_2 \rightarrow CH_2{=}CHCO_2H$) calculated to be an unfavorable +42.7 kJ mol^{-1}.

Introduction

The disposal of carbon dioxide (CO_2) from industrial sources via geosequestration has been identified as a strategy to combat the increasingly important issue of global warming.[1–3] The geosequestration process typically requires separation of CO_2 from the flue gas, followed by compression, and delivery of the purified gas stream to the injection site. This on-tap availability of a cheap and abundant C_1 feedstock represents an excellent opportunity for value adding through conversion of CO_2 to an industrially valuable product.

The use of CO_2 as a potential carbon source has been hampered in general by its chemical inertness. The transformation of CO_2 into other organic compounds, however, can typically be mediated by various transition metals that are able to activate CO_2 or its coupling partner, resulting in the formation of new C−C, C−N, C−O, or C−H bonds.[4–13]

Research has been particularly active in areas that focus on transition-metal-assisted coupling of CO_2 with other readily available feedstocks.[14–17] The coupling of CO_2 with ethylene to form high-demand acrylic acid (Scheme 1) represents an excellent potential target for value adding the CO_2 gas stream. The current industrial technique for synthesis of acrylic acid is energetically expensive due to both the temperature required for efficient catalysis (210–480 °C) and the need for multiple distillations to remove aldehyde impurities.[18,19] More importantly, the technique is not generally amenable to the synthesis of substituted acrylates, with the choice of carbon-based feedstock being limited to propylene.

Scheme 1. Acrylic Acid Formation via Coupling of Carbon Dioxide and Ethylene

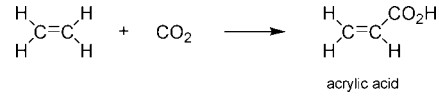

The formation of a metallacycle via transition-metal-assisted coupling of CO_2 with unsaturated hydrocarbons represents an initial step toward synthesis of substituted acrylates. Experimental methods for preparation of these metallacycles have focused primarily on low-temperature homogeneous reactions

* To whom correspondence should be addressed. E-mail: mark.buntine@adelaide.edu.au. Fax: +61 8 8303 4358. Tel: +61 8 8303 5580.

(1) Rubin, E.; Meyer, L.; deConinck, H. Intergovernmental Panel of Climate Change (IPCC) Special Report on Carbon Dioxide Capture and Storage (2005), http://www.ipcc.ch/activity/srccs/.
(2) Thomas, C. D.; Cameron, A.; Green, R. E.; Bakkenes, M.; Beaumont, L. J.; Collingham, Y. C.; Erasmus, B. F. N.; de Siqueira, M. F.; Grainger, A.; Hannah, L.; Hughes, L.; Huntley, B.; van Jaarsveld, A. S.; Midgley, G. F.; Miles, L.; Ortega-Huerta, M. A.; Peterson, A. T.; Phillips, O. L.; Williams, S. E. *Nature* **2004**, *427*, 145–148.
(3) Lackner, K. S. *Science* **2003**, *300*, 1677–1678.
(4) Louie, J. *Curr. Org. Chem.* **2005**, *9*, 605–623.
(5) Braunstein, P.; Matt, D.; Nobel, D. *Chem. Rev.* **1988**, *88*, 747–764.
(6) Leitner, W. *Coord. Chem. Rev.* **1996**, *153*, 257–284.
(7) Yin, X. L.; Moss, J. R. *Coord. Chem. Rev.* **1999**, *181*, 27–59.
(8) Gibson, D. H. *Coord. Chem. Rev.* **1999**, *186*, 335–355.
(9) Palmer, D. A.; van Eldik, R. *Chem. Rev.* **1983**, *83*, 651–731.
(10) Gibson, D. H. *Chem. Rev.* **1996**, *96*, 2063–2095.
(11) Behr, A. *Angew. Chem., Int. Ed. Engl.* **1988**, *27*, 661–678.
(12) Arakawa, H.; Aresta, M.; Armor, J. N.; Barteau, M. A.; Beckman, E. J.; Bell, A. T.; Bercaw, J. E.; Creutz, C.; Dinjus, E.; Dixon, D. A.; Domen, K.; DuBois, D. L.; Eckert, J.; Fujita, E.; Gibson, D. H.; Goddard, W. A.; Goodman, D. W.; Keller, J.; Kubas, G. J.; Kung, H. H.; Lyons, J. E.; Manzer, L. E.; Marks, T. J.; Morokuma, K.; Nicholas, K. M.; Periana, R.; Que, L.; Rostrup-Nielson, J.; Sachtler, W. M. H.; Schmidt, L. D.; Sen, A.; Somorjai, G. A.; Stair, P. C.; Stults, B. R.; Tumas, W. *Chem. Rev.* **2001**, *101*, 953–996.
(13) Aresta, M. *Carbon Dioxide Recovery and Utilization*. Kluwer Academic: Dordrecht, The Netherlands, 2003.
(14) Leitner, W. *Angew. Chem., Int. Ed. Engl.* **1995**, *34*, 2207–2221.
(15) Jessop, P. G.; Ikariya, T.; Noyori, R. *Chem. Rev.* **1995**, *95*, 259–272.
(16) Jessop, P. G.; Joo, F.; Tai, C. C. *Coord. Chem. Rev.* **2004**, *248*, 2425–2442.
(17) Munshi, P.; Main, A. D.; Linehan, J. C.; Tai, C. C.; Jessop, P. G. *J. Am. Chem. Soc.* **2002**, *124*, 7963–7971.
(18) Lin, M. M. *Appl. Catal. A: Gen.* **2001**, *207*, 1–16.
(19) Bettahar, M. M.; Costentin, G.; Savary, L.; Lavalley, J. C. *Appl. Catal. A: Gen.* **1996**, *145*, 1–48.

10.1021/om700592w CCC: $37.00
Publication on Web 11/27/2007

Scheme 2. Transition-Metal-Mediated Coupling of Carbon Dioxide and Ethylene Resulting in a Metallacycle[a]

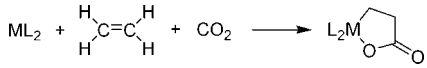

[a] ML_2 = various metal–ligand systems (refer to in-text citations).

involving transition metals such as iron,[20,21] rhodium,[22] zirconium,[23,24] titanium,[25] molybdenum and tungsten,[26–28] and nickel[29–40] (Scheme 2). This experimental work has been supplemented in part by theoretical studies on the coupling reaction, particularly for those systems based on molybdenum[41] and nickel.[42–45]

Further reaction progress beyond the metallacycle toward the formation of an acrylate has been made by Carmona and co-workers for both molybdenum- and tungsten-based precursors.[26,27,41] Their reaction of *trans*-[$M(\eta$-$C_2H_4)_2(PMe_3)_4$] (M = Mo, W) with CO_2 yielded a dimeric metal species bridged by two acrylate units formed via oxidative coupling of CO_2 and ethylene, followed by β-H transfer to the metal center (Scheme 3). Subsequent theoretical calculations involving derivation of the entire potential energy surface[41] confirmed the proposed intermediacy of a metallacycle species, but this species could not be isolated experimentally. Unfortunately, the reaction is unattractive from an industrial synthesis perspective, as the bridged acrylate cannot be easily displaced, and it is not possible to regenerate the initial molybdenum complex.

Scheme 3. Transition-Metal-Mediated Coupling of Carbon Dioxide and Ethylene Resulting in an Acrylate-Bridged Dimer (M = Mo, W)

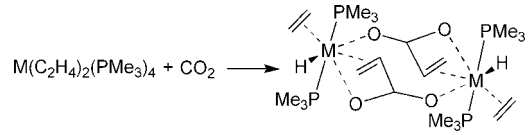

Scheme 4. Nickelacycle Formation and the Alternative Acidification Products Formed Depending on Reaction Temperature

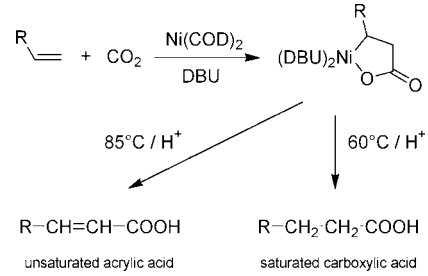

The majority of research on acrylate production from metal-assisted coupling of CO_2 with alkenes or alkynes originates from the nickel-based work of Hoberg and co-workers.[29–37] Their series of papers in the 1980s detailed the formation of saturated and unsaturated carboxylic acids (i.e., acrylates) via the coupling of CO_2 with a variety of alkenes. This coupling reaction was typically mediated by a stoichiometric amount of nickel bis(diazabicyclo[5.4.0]undec-7-ene) ($Ni(DBU)_2$) formed in situ from $Ni(COD)_2$ and DBU (Scheme 4). Formation of the isolable nickel-based metallacycle[37] (i.e., nickelacycle) takes place via coupling of the alkene with CO_2 in tetrahydrofuran (THF) under mild reaction conditions (60 °C). Acidification of the reaction mixture at this temperature results in the formation of a saturated carboxylic acid. Conversely, increasing the temperature to 85 °C is believed to promote β-H elimination, which after acidification furnishes the target acrylate. Both of these reactions are noncatalytic, as they rely on stoichiometric amounts of the nickel reagent, which is oxidized to an unknown nickel(II) species as part of the process.

Hoberg suggested that the expected catalytic activity was not observed in the acrylate case due to a hydride transfer reaction of the hydride ligand from the nickel center to DBU (Scheme 5b).[29,37] This reaction would prevent the desired reductive elimination from taking place, thus inhibiting both the formation of acrylic acid and regeneration of the zerovalent nickel catalyst (Scheme 5a).

In a recent communication,[46] Fischer et al. confirmed the importance of the proposed nickel−acrylate intermediate by isolating the first such species from the β-H elimination of a nickelacycle. Substitution of the spectator ligands on the nickelacycle with bis(diphenylphosphino)methane (dppm) resulted in the formation of a stable binuclear Ni(I) complex with a bridging acrylate ligand. Application of the reaction to a catalytic process is currently hampered by the unwanted cleavage of a PPh_2 group from the dppm ligand and H migration,

(20) Hoberg, H.; Jenni, K.; Kruger, C.; Raabe, E. *Angew. Chem., Int. Ed. Engl.* **1986**, *25*, 810–811.
(21) Hoberg, H.; Jenni, K.; Angermund, K.; Kruger, C. *Angew. Chem., Int. Ed. Engl.* **1987**, *26*, 153–155.
(22) Aresta, M.; Quaranta, E. *J. Organomet. Chem.* **1993**, *463*, 215–221.
(23) Burlakov, V. V.; Arndt, P.; Baumann, W.; Spannenberg, A.; Rosenthal, U. *Organometallics* **2006**, *25*, 1317–1320.
(24) Yamashita, K.; Chatani, N. *Synlett* **2005**, 919–922.
(25) Cohen, S. A.; Bercaw, J. E. *Organometallics* **1985**, *4*, 1006–1014.
(26) Alvarez, R.; Carmona, E.; Cole-Hamilton, D. J.; Galindo, A.; Gutierrez-Puebla, E.; Monge, A.; Poveda, M. L.; Ruiz, C. *J. Am. Chem. Soc.* **1985**, *107*, 5529–5531.
(27) Alvarez, R.; Carmona, E.; Galindo, A.; Gutierrez, E.; Marin, J. M.; Monge, A.; Poveda, M. L.; Ruiz, C.; Savariault, J. M. *Organometallics* **1989**, *8*, 2430–2439.
(28) Galindo, A.; Pastor, A.; Perez, P. J.; Carmona, E. *Organometallics* **1993**, *12*, 4443–4451.
(29) Burkhart, G.; Hoberg, H. *Angew. Chem., Int. Ed. Engl.* **1982**, *21*, 76–76.
(30) Hoberg, H.; Schaefer, D. *J. Organomet. Chem.* **1982**, *236*, C28–C30.
(31) Hoberg, H.; Schaefer, D. *J. Organomet. Chem.* **1983**, *251*, C51–C53.
(32) Hoberg, H.; Peres, Y.; Milchereit, A. *J. Organomet. Chem.* **1986**, *307*, C38–C40.
(33) Hoberg, H.; Peres, Y.; Milchereit, A. *J. Organomet. Chem.* **1986**, *307*, C41–C43.
(34) Hoberg, H.; Ballesteros, A.; Sigan, A. *J. Organomet. Chem.* **1991**, *403*, C19–C22.
(35) Hoberg, H.; Ballesteros, A.; Sigan, A.; Jegat, C.; Barhausen, D.; Milchereit, A. *J. Organomet. Chem.* **1991**, *407*, C23–C29.
(36) Hoberg, H.; Ballesteros, A. *J. Organomet. Chem.* **1991**, *411*, C11–C18.
(37) Hoberg, H.; Peres, Y.; Kruger, C.; Tsay, Y. H. *Angew. Chem., Int. Ed. Engl.* **1987**, *26*, 771–773.
(38) Saito, S.; Nakagawa, S.; Koizumi, T.; Hirayama, K.; Yamamoto, Y. *J. Org. Chem.* **1999**, *64*, 3975–3978.
(39) Takimoto, M.; Shimizu, K.; Mori, M. *Org. Lett.* **2001**, *3*, 3345–3347.
(40) Shimizu, K.; Takimoto, M.; Sato, Y.; Mori, M. *Org. Lett.* **2005**, *7*, 195–197.
(41) Schubert, G.; Papai, I. *J. Am. Chem. Soc.* **2003**, *125*, 14847–14858.
(42) Dedieu, A.; Ingold, F. *Angew. Chem., Int. Ed. Engl.* **1989**, *28*, 1694–1695.
(43) Sakaki, S.; Mine, K.; Hamada, T.; Arai, T. *Bull. Chem. Soc. Jpn.* **1995**, *68*, 1873–1882.
(44) Sakaki, S.; Mine, K.; Taguchi, D.; Arai, T. *Bull. Chem. Soc. Jpn.* **1993**, *66*, 3289–3299.
(45) Papai, I.; Schubert, G.; Mayer, I.; Besenyei, G.; Aresta, M. *Organometallics* **2004**, *23*, 5252–5259.
(46) Fischer, R.; Langer, J.; Malassa, A.; Walther, D.; Gorls, H.; Vaughan, G. *Chem. Commun.* **2006**, 2510–2512.

Scheme 5. Proposed Routes from the Nickelacycle for Production of Acrylic Acid: (a) *Desired* Reductive Elimination Resulting in Production of the Acrylate and Regeneration of the Active Catalyst; (b) *Proposed* Intramolecular H-Transfer Reaction Resulting in the Need for Acid Hydrolysis To Produce the Required Acrylate

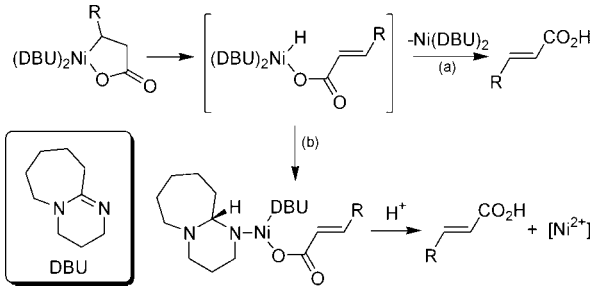

Scheme 6. Synthesis of a Bridged Nickel−Acrylate Species through β-H Elimination from a Nickelacycle[a]

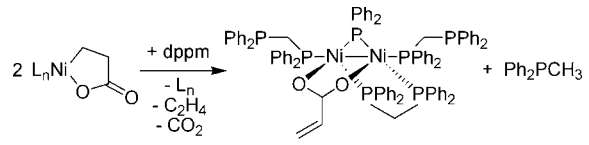

[a] L_n = tmeda, 2-pyridine.

which results in formation of a phosphido bridge (−PPh_2−) and methyldiphenylphosphine (Ph_2PCH_3) (Scheme 6).

Attempts to overcome the noncatalytic nature of the coupling reaction first observed by Hoberg have proven largely unsuccessful. Simple substitution of the spectator ligands would be the intuitive solution, on the basis of the decomposition assumption made by Hoberg, but this approach has resulted in the formation of nickelacycles that do not undergo β-H elimination, except in the presence of a Lewis base. Alternatively, further reaction flexibility has been added by using an *alkyne* in preference to an alkene substrate, allowing the synthesis of *unsaturated* nickelacycle intermediates. This strategy eliminates the need for β-H elimination, as simple acidification can furnish the desired acrylate product. While this strategy protects the catalyst from the intramolecular reaction described earlier, as there is no nickel−hydride species formed, the nickel center must be reduced after each cycle for catalysis to continue. This reduction has been achieved electrolytically using a sacrificial magnesium anode,[47] or as part of a catalytic cycle at the expense of an alkyl−zinc reagent.[40]

True catalytic acrylate generation through coupling of CO_2 with unsaturated hydrocarbons is a goal that, at present, remains elusive. In this study, density functional theory (DFT) is employed to study the desired catalytic coupling reaction between carbon dioxide and ethylene over a $Ni(DBU)_2$ catalyst. The potential energy surface obtained is compared with that for the catalyst deactivation reaction proposed by Hoberg with the ultimate aim of providing a rationale for the experimental observations.

Computational Details

All geometry optimizations were carried out using the B3LYP[48–50] density functional and the LANL2DZ:6-31+G(d,p) compound basis set (consisting of the LANL2DZ basis set[51,52] on nickel and 6-31+G(d,p) basis set[53–56] on the remaining atoms), with pure d functions (5D) used throughout.

Harmonic vibrational frequencies were calculated on the optimized geometries to ascertain the nature of the stationary points with zero-point vibrational energy (ZPVE) and thermodynamic corrections obtained using unscaled frequencies. Additional calculations were performed on all species to ensure the stability of the wave function (stable=opt). For transition structures, the connection between reactants and products was verified by following the normal coordinate corresponding to the imaginary frequency using the Berny optimization algorithm with a reduced maximum step size (psuedo-IRC calculation).

Energy corrections due to solvation were applied to optimized geometries by means of the polarizable continuum model (IEF-PCM)[57–60] using radii based on the United Atom Topological Model (RADII=UAHF). The dielectric constant (ϵ) was set to 7.58 in order to simulate experimental reaction conditions in tetrahydrofuran (THF).

In the reaction surface diagrams, gas-phase Gibbs free energies are represented by solid lines, while solvent-corrected (THF) Gibbs free energies are represented by dashed lines. Relative energies quoted throughout the text are in kJ mol^{-1} and refer to solvation-corrected Gibbs free energies at 298 K unless otherwise specified.

All calculations were carried out using the Gaussian03 suite of programs.[61]

Results

The combination of a large molecular system and a moderately large basis set in the present study comes at significant computational cost. In an effort to reduce this cost, a truncated model of the diazabicyclo[5.4.0]undec-7-ene (DBU) ligand was employed. The model ligand (denoted *m*DBU) has three carbon atoms removed from the seven-membered ring distal to the coordinating nitrogen (Figure 1). Use of this abbreviated system resulted in a time saving of greater than 50% when undertaking frequency calculations.

(47) Derien, S.; Dunach, E.; Perichon, J. *J. Am. Chem. Soc.* **1991**, *113*, 8447–8454.
(48) Becke, A. D. *J. Chem. Phys.* **1993**, *98*, 5648–5652.
(49) Becke, A. D. *Phys. Rev. A* **1988**, *38*, 3098–3100.
(50) Lee, C.; Yang, W.; Parr, R. G. *Phys. Rev. B* **1988**, *37*, 785–789.
(51) Dunning, T. H.; Hay, P. J. *Modern Theoretical Chemistry*. Plenum: New York, 1976; Vol. 3, p 1.
(52) Hay, P. J.; Wadt, W. R. *J. Chem. Phys.* **1985**, *82*, 299.
(53) Hehre, W. J.; Ditchfie, R.; Pople, J. A. *J. Chem. Phys.* **1972**, *56*, 2257 ff.
(54) Hariharan, P. C.; Pople, J. A. *Theor. Chim. Acta* **1973**, *28*, 213–222.
(55) Spitznagel, G. W.; Clark, T.; Chandrasekhar, J.; Schleyer, P. v. R. *J. Comput. Chem.* **1982**, *3*, 363–371.
(56) Clark, T.; Chandrasekhar, J.; Spitznagel, G. W.; Schleyer, P. v. R. *J. Comput. Chem.* **1983**, *4*, 294–301.
(57) Mennucci, B.; Tomasi, J. *J. Chem. Phys.* **1997**, *106*, 5151–5158.
(58) Cances, E.; Mennucci, B.; Tomasi, J. *J. Chem. Phys.* **1997**, *107*, 3032–3041.
(59) Cossi, M.; Barone, V.; Mennucci, B.; Tomasi, J. *Chem. Phys. Lett.* **1998**, *286*, 253–260.
(60) Cossi, M.; Scalmani, G.; Rega, N.; Barone, V. *J. Chem. Phys.* **2002**, *117*, 43–54.
(61) Frisch, M. J.; Trucks, G. W.; Schlegel, H. B.; Scuseria, G. E.; Robb, M. A.; Cheeseman, J. R.; Montgomery, J. A., Jr.; Vreven, T.; Kudin, K. N.; Burant, J. C.; Millam, J. M.; Iyengar, S. S.; Tomasi, J.; Barone, V.; Mennucci, B.; Cossi, M.; Scalmani, G.; Rega, N.; Petersson, G. A.; Nakatsuji, H.; Hada, M.; Ehara, M.; Toyota, K.; Fukuda, R.; Hasegawa, J.; Ishida, M.; Nakajima, T.; Honda, Y.; Kitao, O.; Nakai, H.; Klene, M.; Li, X.; Knox, J. E.; Hratchian, H. P.; Cross, J. B.; Adamo, C.; Jaramillo, J.; Gomperts, R.; Stratmann, R. E.; Yazyev, O.; Austin, A. J.; Cammi, R.; Pomelli, C.; Ochterski, J. W.; Ayala, P. Y.; Morokuma, K.; Voth, G. A.; Salvador, P.; Dannenberg, J. J.; Zakrzewski, V. G.; Dapprich, S.; Daniels, A. D.; Strain, M. C.; Farkas, O.; Malick, D. K.; Rabuck, A. D.; Raghavachari, K.; Foresman, J. B.; Ortiz, J. V.; Cui, Q.; Baboul, A. G.; Clifford, S.; Cioslowski, J.; Stefanov, B. B.; Liu, G.; Liashenko, A.; Piskorz, P.; Komaromi, I.; Martin, R. L.; Fox, D. J.; Keith, T.; Al-Laham, M. A.; Peng, C. Y.; Nanayakkara, A.; Challacombe, M.; Gill, P. M. W.; Johnson, B.; Chen, W.; Wong, M. W.; Gonzalez, C.; Pople, J. A.; *Gaussian 03*, Revision B.05; Gaussian, Inc.: Pittsburgh, PA, 2003.

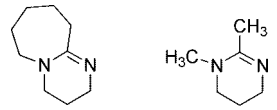

Figure 1. Diazabicyclo[5.4.0]undec-7-ene (DBU) ligand (left) and abbreviated model ligand (*m*DBU) used in this study (right).

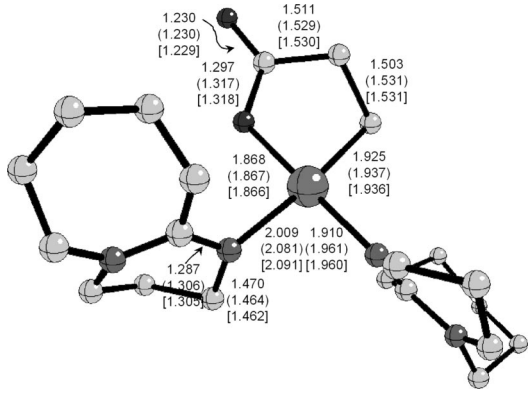

Figure 2. Comparison of experimental crystal data, calculated geometry of the real system (in parentheses), and calculated geometry of the model system (in brackets). All bond lengths are in Å, and hydrogens have been removed from the *m*DBU ligands for clarity.

Comparison of the model ligand with the true ligand system for a small section of the studied electronic energy surface (**III** to **IV**, vide infra) reveals a shift in energy between species of less than 3.6 kJ mol^{-1} (see the Note Added in Proof.Supporting Information). With respect to geometries, the differences observed between the optimized bond lengths in the model and true nickelacycle species were less than 0.01 Å. Further comparison of both sets of geometric data with the crystal structure for the nickelacycle revealed very good reproducibility of the experimental information, confirming the competency of the method used in this study (Figure 2).[37] A recent report[62] citing the benefits of triple-ζ basis sets on nickel recommends use of the B3LYP/SDD:cc-pVDZ//B3PW91/SDD:cc-pVDZ model chemistry,[63–65] especially when changes in the oxidation state of nickel are involved. The performance of the LANL2DZ basis set on nickel was not assessed as part of this investigation. When the recommended model chemistry was tested on the same section of the potential energy surface described previously, it was found that results using our LANL2DZ-based method were within 3.4 kJ mol^{-1} of those obtained via the recommended method (see the>Note Added in Proof.Supporting Information).

The calculated Gibbs free energy surface for the desired nickel-based *catalytic* conversion of CO_2 and ethylene to acrylic acid can be divided into three main sections, each of which will be discussed in detail below.

Nickelacycle Formation. The initial stages of the ethylene/CO_2 coupling reaction leading to nickelacycle formation are relatively well established on the basis of experimental evidence. The proposed $Ni(DBU)_2$ active catalyst is expected to form in situ from $Ni(COD)_2$ and DBU, with oxidative coupling of ethylene and CO_2 substrates resulting in a nickelacycle species that has been isolated and identified by X-ray crystallography.[37]

Scheme 7. First Stage of Nickel-Mediated Ethylene/CO_2 Coupling: Nickelacycle Formation

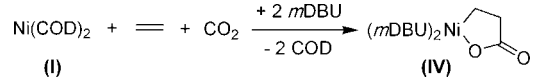

With the exception of the present model DBU ligand (*m*DBU) described above, the species used in modeling this first stage of the coupling reaction replicate the experimental species exactly (Scheme 7).

Using $Ni(COD)_2$, 2 *m*DBU, CO_2, and C_2H_4 as reference points for energies on the free energy surface, the initial ligand exchange from COD to *m*DBU comes at a cost, with $Ni(mDBU)_2$ (**II**) found to lie +61.3 kJ mol^{-1} above $Ni(COD)_2$ (**I**) (Figure 3). A small stabilization is achieved by coordination of ethylene (**III**), although the relative energy of this species is still +36.5 kJ mol^{-1}, suggesting the equilibrium would lie predominantly toward the reactants. It is likely, however, that the initial stages of the reaction will be driven by the exothermic formation of the nickelacycle (**IV**), which is found to lie at −17.2 kJ mol^{-1} relative to reactants.

The barrier to formation of the nickelacycle is calculated to be 121.8 kJ mol^{-1}. The transition structure associated with the barrier (i.e., $\mathbf{TS_{III-IV}}$) exhibits an elongated Ni−C(ethylene) bond on the side of the complex where carbon dioxide resides above the coordination plane (Figure 4). The transition vector corresponding to the imaginary frequency located for $\mathbf{TS_{III-IV}}$ indicates formation of a new C−C bond through attack of the CO_2 carbon on coordinated ethylene combined with concomitant generation of a new Ni−O bond.

The resulting energies and configuration of the transition structure correlate very well with the results of a recent DFT study by Papai et al. examining the analogous nickelacycle formation reaction involving a Ni(bipy) species.[45] Although the theoretical method and initial reaction species differ slightly from those in the present study, the barrier corresponding to nickelacycle formation was calculated to be +79.5 kJ mol^{-1} relative to $Ni(bipy)(C_2H_4)$,[66] which is very similar to the present case (85.3 kJ mol^{-1} relative to **III**).

Although CO_2 coordination to $Ni(mDBU)_2$ was found to be slightly favored over ethylene coordination by 1.7 kJ mol^{-1}, a relaxed potential energy surface scan indicates that the barrier to formation of the nickelacycle through the approach of ethylene on $(mDBU)_2Ni(CO_2)$ is in the vicinity of +85 kJ mol^{-1} higher in energy on the electronic surface than the previously described transition structure for the approach of CO_2 on $(mDBU)_2Ni(C_2H_4)$ (see the Note Added in Proof.Supporting Information). This conclusion is in agreement with Papai, who concluded in that bond formation in the nickelacycle occurs in a single step via the reaction of nickel-coordinated ethylene with an incoming CO_2 molecule.[45]

Nickelacycle to Nickel Acrylate. In comparison to the formation of the nickelacycle—a process that is well established experimentally—the mechanism beyond the nickelacycle leading to the unsaturated acrylic acid remains largely unknown.[67] However, the proposal by Hoberg relating to the existence of a nickel−hydrido−acrylate species on the pathway between the

(62) Ohnishi, Y. Y.; Nakao, Y.; Sato, H.; Sakaki, S. *J. Phys. Chem. A* **2007**, *111*, 7915–7924.
(63) Perdew, J. P.; Wang, Y. *Phys. Rev. B* **1992**, *45*, 13244–13249.
(64) Dunning, T. H. *J. Chem. Phys.* **1989**, *90*, 1007–1023.
(65) Dolg, M.; Wedig, U.; Stoll, H.; Preuss, H. *J. Chem. Phys.* **1987**, *86*, 866–872.

(66) The authors state that on the basis of high-level benchmarking calculations, DFT overestimates this barrier by approximately 20%.[45]
(67) A number of alternate reactions from the nickelacycle have been reported, including further reactions with ethylene that are outside the scope of this study. Only acrylate formation is considered here.

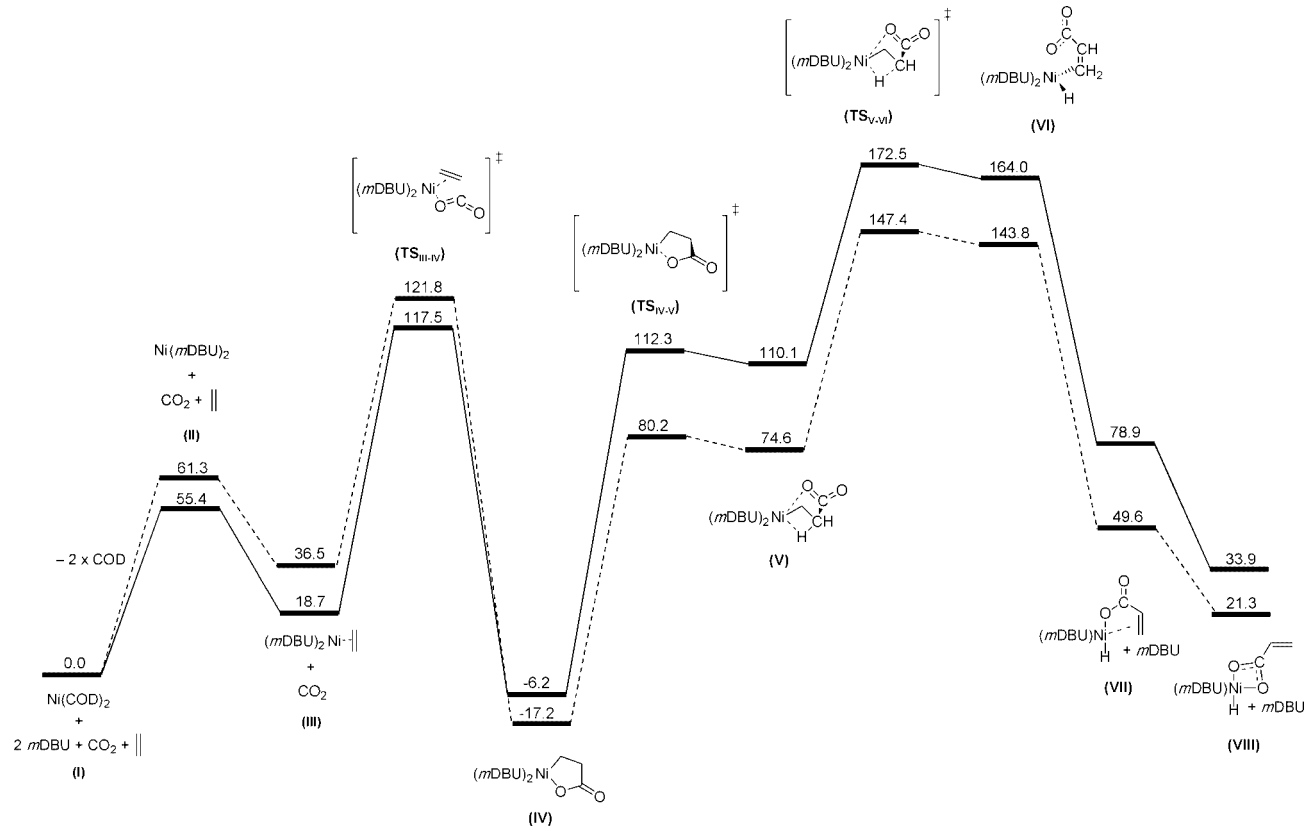

Figure 3. Gibbs free energy surface for first two stages of nickel-mediated coupling of carbon dioxide and ethylene: (1) nickelacycle formation (**I**−**IV**); (2) nickelacycle to nickel acrylate (**IV**−**VIII**). Gas-phase Gibbs free energies (solid line) and solvent-corrected (THF) Gibbs free energies (dashed line) are given in kJ mol^{-1}.

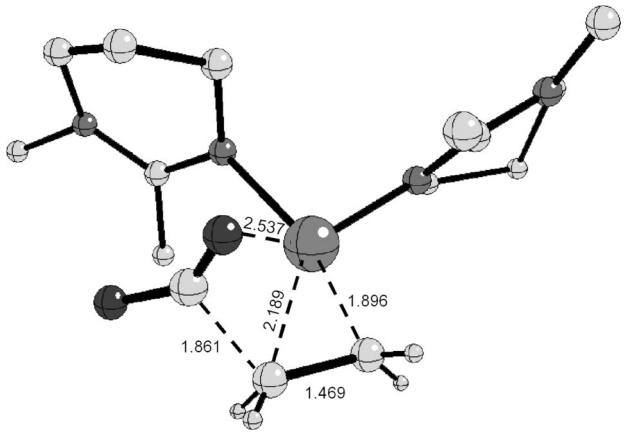

Figure 4. Optimized transition structure geometry for $\mathbf{TS_{III-IV}}$ species. All bond lengths are in Å, and hydrogens have been removed from the *m*DBU ligands for clarity.

nickelacycle and acrylic acid has considerable merit. If β-H elimination were to occur from the nickelacycle, the resulting intermediate would contain both hydride and acrylate ligands. The existence of such a species is reinforced by the recent experimental isolation of a stable nickel−acrylate species via β-H elimination from a nickelacycle (Scheme 6).[46] The lowest energy nickel−hydrido−acrylate species that could be located (**VIII**) is shown in Scheme 8. This species, which contains an acrylate group ligated through both oxygen atoms, is lower in energy than similar structures with alternate coordination modes of acrylate, as well as those containing two *m*DBU ligands in the coordination sphere (see the Note Added in Proof.Supporting Information).

Scheme 8. Second Stage of Nickel-Mediated Ethylene/CO_2 Coupling: Nickelacycle to Nickel Acrylate

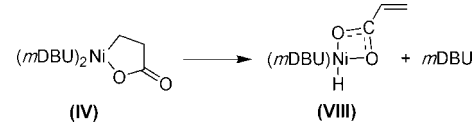

On the basis of the species that are in solution, there exist a number of possible routes from the nickelacycle (**IV**) to the nickel−hydrido−acrylate (**VIII**). As previously described, the simplest mechanism that can be envisaged for the formation of **VIII** involves β-H elimination from the nickelacycle, combined with pre- or post-dissociation of the *m*DBU ligand. The strain imposed by the five-membered nickelacycle, however, makes a suitable geometry from which elimination can occur very difficult to achieve. The search for a transition structure corresponding to direct β-hydrogen elimination from both the four- and three-coordinate (minus one *m*DBU ligand) nickelacycles proved unsuccessful. The restricted conformation imposed by the nickel-oxygen bond means that the α-carbon, β-carbon, and β-hydrogen are unable to adopt a position coplanar with the nickel coordination plane, which is a prerequisite for β-hydrogen elimination from square-planar complexes.

With β-H elimination from the rigid nickelacycle improbable, a number of alternative pathways that may ultimately lead to the nickel−hydrido−acrylate species were considered. The availability of a basic species in solution (i.e., DBU) means that a range of reactions beyond simple cleavages and rearrangements of the nickelacycle is possible (Scheme 9).

Despite the substantial basicity of *m*DBU, abstraction of the tightly bound α- and β-hydrogens of the nickelacycle is energetically unfavorable, with both reactions calculated to be

Scheme 9. Alternative Nickelacycle Reactions That May Ultimately Lead to Formation of Nickel−Hydrido−Acrylate Species (Not Shown)

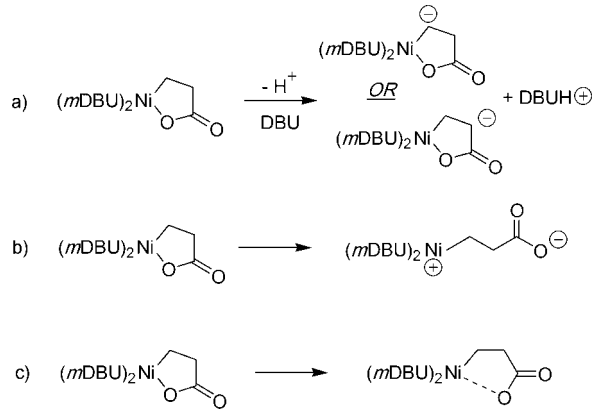

endothermic by more than +450 kJ mol^{-1} on the electronic energy surface (Scheme 9a). Complete cleavage of the nickel−oxygen bond is also difficult (Scheme 9b), with the reaction endothermic by more than +150 kJ mol^{-1} and a barrier in excess of 200 kJ mol^{-1}. Nevertheless, *partial* dissociation of the oxygen from the nickel center may be possible (Scheme 9c), resulting in a minimum (**V**) lying 91.8 kJ mol^{-1} above the nickelacycle (+74.6 kJ mol^{-1} relative to the reactants) on the free energy surface. The structure is characterized by an elongated Ni−O bond (2.74 Å) and an agostic interaction between the β-H and the nickel center. Formation of this species occurs via rotation of the nickelacycle $C_\alpha-C_\beta$ bond and proceeds through a late transition structure ($\mathbf{TS_{IV-V}}$, Figure 5) located +80.2 kJ mol^{-1} relative to the reactants. The transition vector associated with the imaginary frequency of the transition structure corresponds to a twisting of the $C_\alpha-C_\beta$ bond coupled with elongation and contraction of the Ni−O bond. It was envisaged that the partial dissociation of oxygen in **IV** might be aided by the coordination of a solvent molecule (THF) to the metal center. However, the steric bulk in the coordination sphere resulting from two *m*DBU ligands makes the approach of a THF moiety energetically unfavorable.

The partial dissociation of oxygen from the nickel center relieves the steric strain introduced by the five-membered ring and improves accessibility around the coordination sphere, allowing the required coplanarity for β-hydrogen elimination. β-H elimination from **V** results in a species with a new Ni−H bond and an acrylate ligand η^2-bound through the newly formed *C*═C double bond (**VI**). This species is formed via a transition structure (Figure 6, $\mathbf{TS_{IV-V}}$) that has a relative energy of +147.4 kJ mol^{-1}.

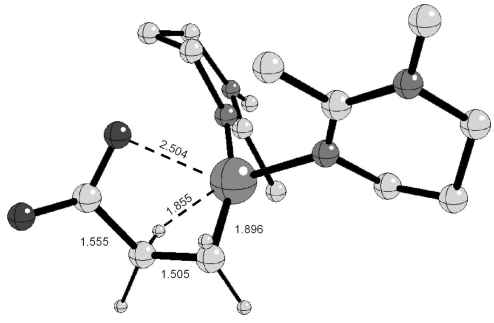

Figure 5. Optimized transition structure geometry for $\mathbf{TS_{IV-V}}$ species. All bond lengths are in Å, and hydrogens have been removed from the *m*DBU ligands for clarity.

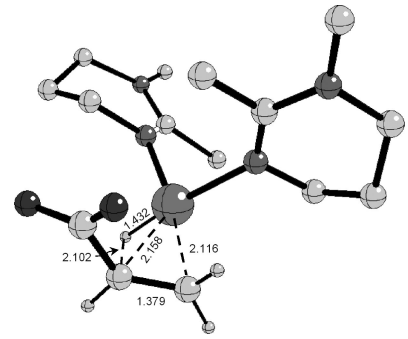

Figure 6. Optimized transition structure geometry for $\mathbf{TS_{V-VI}}$ species. All bond lengths are in Å, and hydrogens have been removed from the *m*DBU ligands for clarity.

Scheme 10. Third Stage of Nickel-Mediated Coupling of Ethylene and CO_2: Removal of Acrylic Acid and Completion of Catalytic Cycle

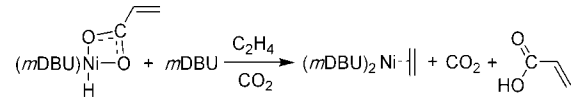

Scheme 11. Possible Avenues for Reductive Elimination of Acrylic Acid from Nickel−Hydrido−Acrylate: Three-Center−Three-Ligand (Pathway A), Five-Center−Three-Ligand (Pathway B), Five-center−Four-Ligand (Pathway C), and Three-Center−Four-Ligand (Pathway D)

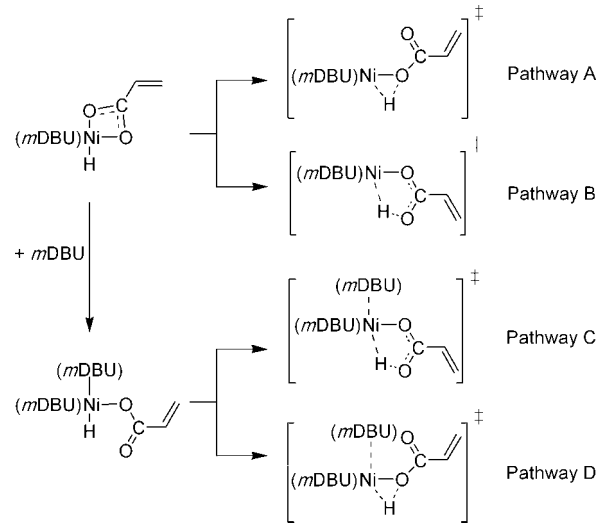

Dissociation of an *m*DBU ligand from the η^2-bound acrylate (**VI**) occurs via a negligible barrier to form a species where the fourth coordination site is now occupied by an acrylate oxygen (**VII**). Subsequent rearrangement then yields the target nickel–hydride–acrylate species (**VIII**), which lies +21.3 kJ mol^{-1} above the reactants.

Liberation of Acrylic Acid. Obtaining acrylic acid catalytically from the nickel−hydrido−acrylate species (**VIII**) requires reductive elimination of the acrylate and hydride ligands (as acrylic acid) with concomitant regeneration of the nickel(0) catalyst. The addition of further ethylene and CO_2 substrates completes the catalytic cycle that began with species **III** (Scheme 10).

Formation of acrylic acid from the nickel−hydrido−acrylate species (**VIII**) and regeneration of the active catalyst is an endothermic process, where the products lie +54.8 kJ mol^{-1}

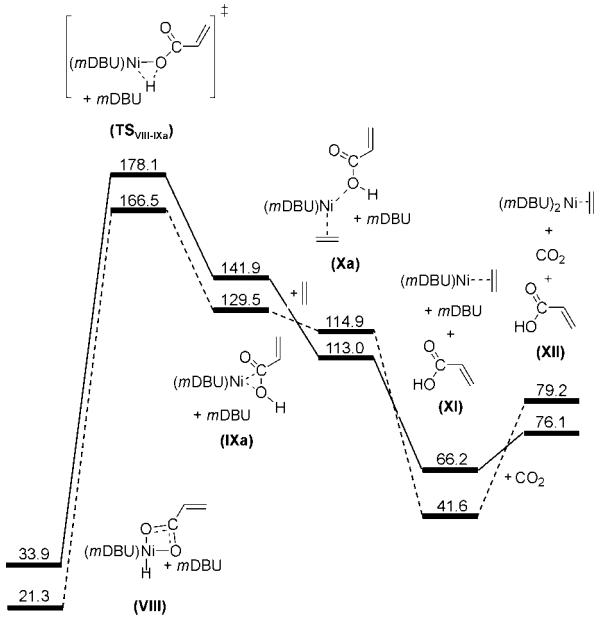

Figure 7. Gibbs free energy surface for the removal of acrylic acid from nickel−acrylate species: pathway A, three-center−three-ligand reductive elimination. Energies are given in kJ mol^{-1}.

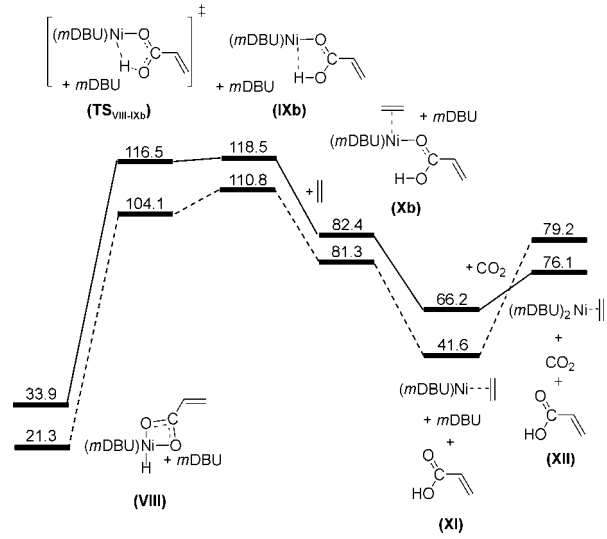

Figure 8. Gibbs free energy surface for the removal of acrylic acid from nickel acrylate species: pathway B, five-center−three-ligand reductive elimination. Energies are given in kJ mol^{-1}.

above **VIII** and +79.2 kJ mol^{-1} relative to the initial reactants on the free energy surface. This unfavorable reaction energy is a manifestation of the endothermic nature of the overall coupling reaction (refer to Scheme 1), which is calculated to have a solvent-corrected Gibbs free energy of +42.7 kJ mol^{-1} (+57.4 kJ mol^{-1} in the gas phase). The calculated gas-phase reaction free energy compares well to the value calculated for the analogous reaction using experimentally derived thermodynamic data: i.e., 50.3 kJ mol^{-1}.[68,69]

The final reductive elimination reaction required to furnish acrylic acid from the nickel−hydrido−acrylate species may occur via a number of avenues. Formation of the new acrylate O−H bond is possible from both three- and four-ligand species (containing one and two *m*DBU ligands, respectively) and may involve the oxygen atom that is either bound to or distal to the metal center (Scheme 11).

Reductive elimination from the three-ligand species involving coupling of the hydride ligand with the nickel-bound acrylate oxygen (pathway A) occurs via a three-centered transition structure with a relative energy of +166.5 kJ mol^{-1} (Figure 7). The resultant product has a relative energy of +129.5 kJ mol^{-1} and corresponds to a species where the acrylate interacts with the nickel center through its C−O bond (**IXa**). Following an associative mechanism, the barrierless addition of ethylene to **IXa** results in the formation of species **Xa**, where the acrylic acid is loosely bound through the hydroxyl oxygen. Subsequent removal of acrylic acid via a minimal barrier[70] furnishes **XI**, which on addition of CO_2 and recoordination of the second *m*DBU ligand regenerates the catalytically active species **XII** (equivalent to **III** plus acrylic acid). Although the regeneration of species **XII** from **XI** is not energetically favorable, the second *m*DBU ligand in the coordination sphere is necessary for progression through the subsequent transition structure (**TS$_{III-IV}$**) and stabilization of the resultant nickelacycle (**IV**) (see the Note Added in Proof.Supporting Information).

Reductive elimination from the three-ligand species may also proceed via coupling of the hydride ligand to the acrylate oxygen that is not bound to the nickel center (pathway B). This route results in a five-centered transition structure with a relative energy of 104.1 kJ mol^{-1} (Figure 8). The O−H coupled product (**IXb**) is still loosely bound to the nickel center via the carboxylate oxygen and is slightly higher in energy than the transition structure on the Gibbs free energy surface.[71] The profile of the reaction then proceeds similarly to that outlined above for pathway A.

Reductive elimination may also take place from a four-coordinate species generated through addition of an *m*DBU ligand to the nickel−hydrido−-acrylate (**VIII**). Coupling of the hydride ligand with the acrylate oxygen distal to the nickel center (pathway C) results in a five-centered transition structure with a relative energy of 186.3 kJ mol^{-1} (Figure 9). The significant increase in the energy of this transition structure over the analogous structure in the three-ligand case is most likely due to the steric hindrance imposed by the additional *m*DBU ligand; however, on the basis of previous research, an electronic preference for the three-ligand pathway is also likely.[72–75] An additional symptom of the introduced steric bulk is the elongation of the bond between the *m*DBU trans to the hydride ligand and the metal center (2.45 Å) and the absence of the second *m*DBU ligand in the coordination sphere of the resulting product (**IXc**). The route to regenerating the active catalyst then proceeds in a fashion identical with that described above for both pathways A and B.

(68) Linstron, P. J.; Mallard, W. G. *NIST Chemistry WebBook, NIST Standard Reference Database Number 69*; National Institute of Standards and Technology: Gaithersburg, MD, 2005; http://webbook.nist.gov.

(69) The standard molar entropy in the gas phase ($S°_{gas}$) was unavailable for acrylic acid. The computed value of 299.0 J/mol K was used.

(70) Assessment of the barrier for removal of acrylic acid was carried out via a potential energy surface scan revealing a barrier of less than 5 kJ mol^{-1} for removal of acrylic acid from **Xa** and less than 20 kJmol^{-1} for removal from **Xb** and **Xc**. Accounting for entropy on the free energy surface would make these fragmentation barriers even less significant.

(71) Although it is indeed a minimum on the electronic surface at the optimization level of theory.

(72) Musashi, Y.; Sakaki, S. *J. Am. Chem. Soc.* **2000**, *122*, 3867–3877.

(73) Tatsumi, K.; Nakamura, A.; Komiya, S.; Yamamoto, A.; Yamamoto, T. *J. Am. Chem. Soc.* **1984**, *106*, 8181–8188.

(74) Tatsumi, K.; Hoffmann, R.; Yamamoto, A.; Stille, J. K. *Bull. Chem. Soc. Jpn.* **1981**, *54*, 1857–1867.

(75) Komiya, S.; Albright, T. A.; Hoffmann, R.; Kochi, J. K. *J. Am. Chem. Soc.* **1976**, *98*, 7255–7265.

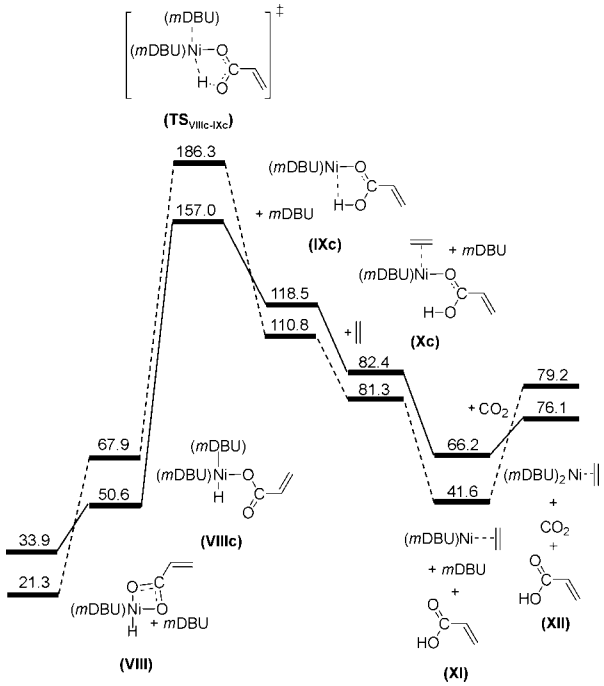

Figure 9. Gibbs free energy surface for the removal of acrylic acid from nickel acrylate species: pathway C, five-center−four-ligand reductive elimination. Energies are given in kJ mol^{-1}.

No transition structure could be located for the four-ligand species, in which O−H coupling takes place between the hydride and the oxygen bound to the nickel center (pathway D). On the basis of the trends observed from the three previous potential energy surfaces, however, the energy of the three-center−four-ligand transition structure is likely to be higher than that of the analogous three-center−three-ligand transition structure, thus making pathway B the lowest energy pathway of those considered.

A dissociative, rather than the previously described associative, pathway was also investigated for the elimination of acrylic acid from species **VIII**. However, removal of acrylic acid from **IX** without prior coordination of ethylene leads to a high-energy coordinatively unsaturated nickel species that makes this route unfavorable (see the Note Added in Proof.Supporting Information).

In summary, the overall catalytic reaction to form acrylic acid through CO_2 and ethylene coupling can be described as having three main stages. Exothermic formation of the nickelacycle (**IV**, −17.2 kJ mol^{-1}) drives the initial induction steps of the reaction and includes overcoming a barrier of +121.8 kJ mol^{-1}. This barrier corresponds to a transition structure that is characterized by the attack of CO_2 on nickel-coordinated ethylene. From the nickelacycle, elongation of the Ni−O bond precedes β-H elimination through a transition structure located at +147.4 kJ mol^{-1}, resulting in a nickel−hydrido−acrylate species in which the acrylate moiety is bound through both oxygens (**VIII**, +21.3 kJ mol^{-1}). The final reductive elimination of acrylic acid from **VIII** may occur via a number of avenues, the lowest energy of which takes place via a five-centered transition structure (+104.1 kJ mol^{-1}) involving the coupling of the hydride ligand with the unbound oxygen of the acrylate ligand.

The overall reaction free energy relative to the reactants is calculated to be endothermic by 79.2 kJ mol^{-1}, with the catalytic portion of the reaction (from **III** to **XII**) endothermic by 42.7 kJ mol^{-1}.

Scheme 12. Possible Routes for Deactivation of Nickel–Hydrido−Acrylate Species via Hydride Migration to the *m*DBU Ligand (a) from Three-Ligand Species, (b) from Four-Ligand Cis Species, and (c) from Four-Ligand Trans Species

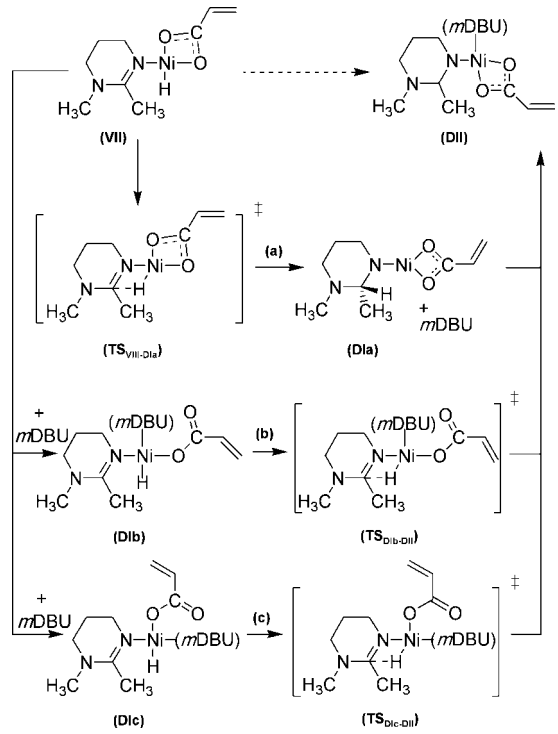

Catalyst Deactivation Route. If the reaction is to adhere to the previously described catalytic route, more favorable reactions outside the desired route must not take place. According to the earlier described proposal by Hoberg, a facile intramolecular reaction takes place, rendering the nickel species unable to accept further substrate and thus preventing catalysis. The deactivation reaction is believed to occur with a nickel−hydrido–acrylate species and involves migration of the hydride ligand to the imine carbon contained in the ring of the adjacent DBU ligand (refer to Scheme 5b). If this deactivation reaction were to take place, the hydride ligand would no longer be available for reductive coupling with the acrylate ligand, preventing both production of acrylic acid and regeneration of the active catalyst.

Much like the reductive elimination reaction required for liberation of acrylic acid described in the previous section, migration of the hydride ligand onto DBU may also take place via a number of avenues (Scheme 12).

Hydride migration from the three-ligand nickel acrylate species (**VIII**) via pathway a is calculated to proceed via a moderate barrier (+150.2 kJ mol^{-1}), affording an end product that is very unstable relative to the initial reactants (Table 1). The stability of the **DIa** product (+111.8 kJ mol^{-1}) is improved slightly by the addition of a further *m*DBU ligand (**DII**, +102.6 kJ mol^{-1}). The addition of a second *m*DBU ligand, however, results in significant destabilization (+203.7 kJ mol^{-1}) attributable to steric crowding.

The intramolecular hydride transfer reaction from a four-coordinate species (containing two *m*DBU ligands) results in one of two additional pathways depending on the position of the newly added *m*DBU ligand. Hydride transfer from the four-ligand species in which the *m*DBU ligands are arranged in a *cis* configuration (pathway b) results in a barrier of +165.4 kJ mol^{-1}, and ultimately leads to the same unstable **DII** species. Hydride migration from the four-ligand *trans* species via the remaining pathway (pathway c) results in a barrier of +181.7

Table 1. Gibbs Free Energy Surfaces for Deactivation of Nickel Catalyst through Hydride Migration from Species VIII[a]

	a	b	c
VIII	21.3 (33.9)	21.3 (33.9)	21.3 (33.9)
$TS_{VIII-DIa}$	150.2 (149.1)		
DIa	111.8 (113.8)		
DIb		67.9 (50.6)	
$TS_{DIb-DII}$		165.4 (141.2)	
DIc			55.7 (31.7)
$TS_{DIc-DII}$			181.7 (163.9)
DII	102.6 (81.0)	102.6 (81.0)	102.6 (81.0)

[a] The column heads a−c refer to the pathways in Scheme 12. Solvent-corrected Gibbs free energies are given in kJ mol^{-1} (gas-phase energies are shown in parentheses).

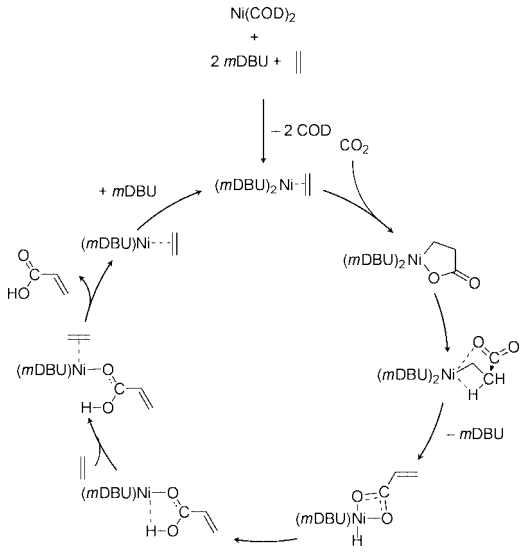

Figure 10. Proposed catalytic cycle for the coupling of CO_2 and ethylene to produce acrylic acid.

kJ mol^{-1}, which is higher in energy than both the four-ligand *cis* and three-ligand pathways. Therefore, if hydride migration is to occur from the nickel−hydrido−acrylate species, a barrier of 150.2 kJ mol^{-1} must be overcome. The resultant product is not particularly stable, having an energy of +102.6 kJ mol^{-1} relative to the initial reactants.

Conclusions

Calculation of the Gibbs free energy surfaces for both the catalytic coupling of CO_2 and ethylene and the proposed deactivation reaction of the nickel catalyst gave a number of insights with regard to the experimental observations reported by Hoberg.

The calculated nickel-mediated catalytic cycle (Figure 10) appears to be hindered not by unsurmountable barriers or the proposed deactivation reaction but as a result of the overall thermodynamics of the coupling reaction. The catalytic reaction is subject to three main barriers: nickelacycle formation (+121.8 kJ mol^{-1}), β-H elimination (+147.4 kJ mol^{-1}), and reductive elimination of acrylic acid through a five-center−three-ligand transition structure (+104.1 kJ mol^{-1}). As the β-H elimination reaction is observed experimentally to take place at 85 °C, none of these barriers would be expected to hinder the progress of the catalytic reaction. The deactivation reaction proposed by Hoberg in order to justify the lack of observed catalytic activity is subject to a moderate barrier (+150.2 kJ mol^{-1}), but it is the instability of the product (+102.1 kJ mol^{-1}) that reduces the likelihood of the reaction taking place. The lack of observed catalytic activity is far more likely to be a symptom of the free energy of reaction, which is calculated to be +79.2 kJ mol^{-1}. The overall reaction free energy, including both the entrance into the catalytic cycle (**I**−**III**) and the cycle itself (**III**−**XII**) is a manifestation of the free energy change of the $CO_2 + C_2H_4 \rightarrow CH_2CHCO_2H$ coupling reaction, which is calculated to be +42.7 kJ mol^{-1}.

On the basis of the above results, it is possible that catalytic formation of acrylic acid may well have been occurring in the original reaction, although the overall thermodynamics create an unfavorable equilibrium that would lead to undetectable amounts of the acrylic acid.

The temperature dependence of the observed hydrolysis products can be explained on the basis of the barriers calculated for the reaction. At 60 °C, the barrier to nickelacycle formation (+121.8 kJ mol^{-1}) can be overcome, with acidification of the nickelacycle (**V**) furnishing the experimentally observed saturated carboxylic acid. Increasing the temperature to 85 °C also allows traversal of the subsequent barrier to β-H elimination (+141.7 kJ mol^{-1}). At this temperature, the observed liberation of the acrylate through acidification is likely to take place from the nickel−hydrido−acrylate species (**VIII**) in preference to the proposed alternate precursor (**DII**), which is ca. 80 kJ mol^{-1} less stable.

It is important that any future efforts that focus on the catalytic synthesis of acrylic acid from CO_2 and ethylene deal with the unfavorable free energy of the overall coupling reaction. Possible solutions may include preventing the reaction from reaching equilibrium through removal of the product from solution or reacting the acrylic acid further to improve the overall thermodynamics. Further theoretical work is being undertaken in order to investigate these strategies.

Acknowledgment. We thank the Radom group at the University of Sydney for their kind hospitality. We are also indebted to both the Australian Partnership for Advanced Computing (APAC) and South Australian Partnership for Advanced Computing (SAPAC) for generous time grants on their parallel computing facilities.

Note Added in Proof. Fast elimination of acrylate esters formed by insertion of ethylene into a pre-formed Pd–CO_2Me bond has been recently reported. Aresta, M.; Pastore, C.; Giannoccaro, P.; Kovacs, G.; Dibenedetto, A.; Papai, I. *Chem. Eur. J.* **2007**, *13*, 9028–9034.

Supporting Information Available: Tables and figures giving optimized geometries, thermodynamic and solvation corrections, and single-point energies. This material is available free of charge via the Internet at http://pubs.acs.org.

OM700592W